4open 2022, **5**, 19

https://doi.org/10.1051/fopen/2022021

4 Open

Available online at:
www.4open-sciences.org

Special issue of 4open on Inorganic Nanoparticle Luminophore: Design and Application

RESEARCH ARTICLE OPEN ACCESS

Synthesis and characterization of Inorganic Nanoparticles Luminophores for Environmental Remediation

Abdul Aziz Shaikh[1,a], Souhardya Bera[2,a], Swastik Paul[2,a], Shibsankar Mondal[2,a], Ankit Saha[2,a], and Subhasis Roy[2,a,*]

[1] Integrated Science Education and Research Centre (ISERC), Visva-Bharati University, Santiniketan, West Bengal 731235, India
[2] Department of Chemical Engineering, University of Calcutta, 92 A.P.C. Road, Kolkata 700009, India

Received 6 July 2022, Accepted 20 October 2022

Abstract – Inorganic Nanoparticle Luminophores have been the focus of ongoing research because of their special characteristics as they approach nanoscale from bulk nature. Besides, their application remains highly diverse compared to bulk zero-valent metals. In this research work, facile and economical borohydride reduction of ferric chloride was undertaken to study the kinetics of phenol photodegradation under simulated sunlight conditions. Further, photoluminescence study was undertaken to calculate the lowest energy transition of our synthesized sample. The synthesized NPs were analyzed using XRD. SEM and TEM data showed the presence of an interconnected network of nanospheresof uniform morphology in the particle range of 20–60 nm, with formation of long-chain of aggregates-characteristic of mixed valent iron oxides, which predominates on a rapidly oxidizing nZVI particle system. The photodegradation studies showed a promising result, degrading nearly the complete concentration of phenol within 24 hours. PL study reported the lowest energy transition at 1.72 eV which alternatively confirms its application as a photocatalyst in diverse fields of wastewater remediation.

Keywords: Inorganic Nanoparticle Luminophores, nZVI, Photodegradation, Photoluminescence

Introduction

The presence of phenolic component effluents in heavy manufacturing industries namely oil refining and petrochemicals, pulp, paper, paint, and pharmaceutical renders serious health hazards to aquatic life and subsequently to mankind. The released phenol can get rapidly absorbed through contact with human skin and can cause health issues both acute and chronic ranging from subdued irritation and coughing to neuropsychiatric disturbance and respiratory arrest. Phenol has been classified as a priority pollutant by the United States Environmental Protection Agency (EPA) and other international regulatory bodies and the maximum allowable concentration has been set to be less than 5 mg/L, whereas human consumption of more than 1 g/L of the same proves to be fatal. However, the phenol concentration, for example, from the petroleum industry varies from 0.1 to 0.017 mg/L. Moreover, phenol and its derived compounds in wastewater possess a natural inhibitory effect on the general biological treatment performed by micro-organisms. It is, therefore, imperative that industrial wastewater undergoes extensive treatment before being released to natural water bodies. Fungi and bacteria have been studied extensively for the removal of phenolic compounds whereas efforts have been also made to test algae for the same [1, 2].

The phenol removal capacity of engineered nanoscale zero-valent iron (nZVI) and its variation in wastewater remediation, especially in the class of heavy metals and organic compounds, is solely due to its high reactivity and catalytic capability compared to zero-valent metals (ZVMS) especially here in the case of (ZVIs) dimensional reduction provides increasing reagent reactivity which is imperative due to the contact surface area enhancement. However, the mechanism of removal of the dissolved organic compounds remains unresolved to date. The potential increase in the chemical reactivity also provides higher and significant kinetic gain [3]. Additionally, nanoparticle-based metal atoms prove superior over conventional wastewater treatment processes for their uneconomical and energy-intensive exercise. Therefore, there remains restricted use of these large-scale conventional operations. Herein, in theory, iron-based nanoparticles provide greater prospects because of their abundance and their low cost. Moreover, the removal capacity of metal ions such as Cu^{2+}, Ba^{2+}, Cr^{2+}, and Pb^{2+} is prosperous in terms of their removal efficiency [4, 5].

Bottom-up approaches such as precipitation [6], hydrogenation [7], and chemical reduction [8] have been used to make zero-valent iron nanoparticles in recent decades.

*Corresponding author: subhasis1093@gmail.com, srchemengg@caluniv.ac.in
[a]All the authors have contributed equally.

The borohydride reduction method is the most extensively used method for synthesizing nZVI. The following reaction equation shows the synthesis of nZVI using $NaBH_4$.

$$2FeCl_3 + 6NaBH_4 + 18H_2O \rightarrow 2Fe^0 + 6NaCl + 6B(OH)_3 + 21H_2 + 6NaCl. \quad (1)$$

Surface and groundwater may be contaminated by wastewater created by industry. As a result, it has the potential to have negative consequences for aquatic life as well as human health. Phenol has high toxicity to human health as it has limited biological breakdown capability and high carcinogenic and mutagenic nature [9, 10]. The removal of this chemical and its derivatives from industrial wastewater is a problem for the environment. Biosorption, chemical oxidation with ozone, adsorption, ion exchange, photodegradation [11], membrane separation, active carbon, and other approaches have been used to remove phenol from water wastewater [12]. Most of these approaches tend to be costly and may produce sludge, which is difficult to dispose of [13].

However, regardless of their contaminant removal and phenol degrading capability, their efficiency has not been well documented. Additionally, a plethora of research papers has been published reporting a variety of synthesis processes which however have carried out the reduction process using an aqueous medium. However, it is imperative that nVZI would undergo massive oxidation under open air, and therefore a change of medium might be an effective way to prohibit the same. Since, the chemical reduction approach helps create a homogenous structure, thereby displaying higher reactivity [14]. This research focuses on use of ethanol as the medium, and the further characterization of the synthesized (nVZI) material to derive an idea about its surface properties and size. The optical properties and transition energy were investigated using photoluminescence absorption spectra, due to the relative difficulty in attaining the UV–Vis spectra of insoluble nZVI particles. Experimentally obtained XRD patterns were analyzed to understand the lattice structure of (nZVI) nanoparticles. Field Emission scanning electron microscopy (FESEM) and Transmission electron microscopy (TEM) helped characterize the surface morphology and particle size distribution and uniformity respectively. The ethanol medium-based experimentally synthesized (nZVI), NPs were then used to test their efficiency in the photodegradation of organic compounds, in this case, phenol. The catalyst was also recovered by filtration, and studied for its reusability. In order to comprehend the sample's charge transfer properties and identify the lowest energy transition, PL investigations were also acquired.

Materials and methods

Chemicals and reagents

The required materials have been procured and put to use without any further purification. Ferric chloride hexahydrate ($FeCl_3 \cdot 6H_2O$) (LobaChemie, India), Sodium borohydride ($NaBH_4$) (Winlab Co., UK), Ethanol, Whatman Filter Paper No. 1, MB (Farbwerke Hoechst AG; BP 58 Germany).

Synthesis of nZVI

As reported previously, nZVI nanoparticles were synthesized utilizing a simple chemical reduction method under atmospheric conditions [15]. The synthesis of zero-valent iron nanoparticles was carried out using sodium borohydride as a reducing agent in an ethanol medium. Two solutions named "Solution A" and "Solution B" were prepared.

"Solution A" was synthesized using $FeCl_3 \cdot 6H_2O$ (0.5M) in a 4:1 ratio of ethanol and water. Stoichiometric amounts of ferric chloride hexahydrate were dissolved in ethanol and De-Ionized (DI) water and were stirred continuously for 1 hr. "Solution B" was prepared using $NaBH_4$ (1M) and DI. Further, Solution A was kept under continuous stirring and Solution B was added dropwise. With the first drop, a black color precipitate was observed. The whole experiment was carried out inside a fume hood to drain out the hydrogen gas evolved. The black precipitate formed was filtered out using vacuum filtration and Whatman Filter Paper No. 1. Additionally, the precipitate was washed twice with ethanol to avoid the oxidation of nZVI. Finally, the synthesized particles were dried in a vacuum oven overnight and stored with the help of ethanol to avoid oxidation.

Results and discussions

XRD study of (nZVI) was performed to identify the phases of our synthesized (nZVI) nanoparticle employing Cu-kα source and graphite monochromator to produce a wavelength of 1.54 Å. The XRD (Philips Analytical PW 3050/60X'Pert Pro) experiment was carried out on freshly derived nZVI NPs to mitigate their inherent problem of forming new mineral phases with progressive aging. The sample was however heated first to evaporate the ethanol out which was added to mitigate the problem of oxidation of nZVI NPs.. Additionally, the experimentally obtained XRD showed definite and distinct peaks that made the qualitative and quantitative contributions of the mineral phases possible. The XRD analysis of our nZVI NPs has been plotted without any refinement and is shown in Figure 1. The sample demonstrated prominent high-intensity peaks at $2\theta = 45.38^{\circ}$ and 59.30° – characteristics of pure-phased Fe^0 nanoparticles [16, 17]. The additional indexed peaks can be understood as contributions from mixed valent iron oxides – Fe_2O_3 and Fe_3O_4. Respective peak intensities indicate the role of temperature in the formation of the nZVI phase. The grain size of our sample was calculated using the Scherrer equation:

$$\beta = \frac{0.9\lambda}{D\cos\theta}, \quad (2)$$

where, "$\boldsymbol{k}$" is the Cu–kα radiation wavelength, i.e., 1.54 Å or 0.154 nm.

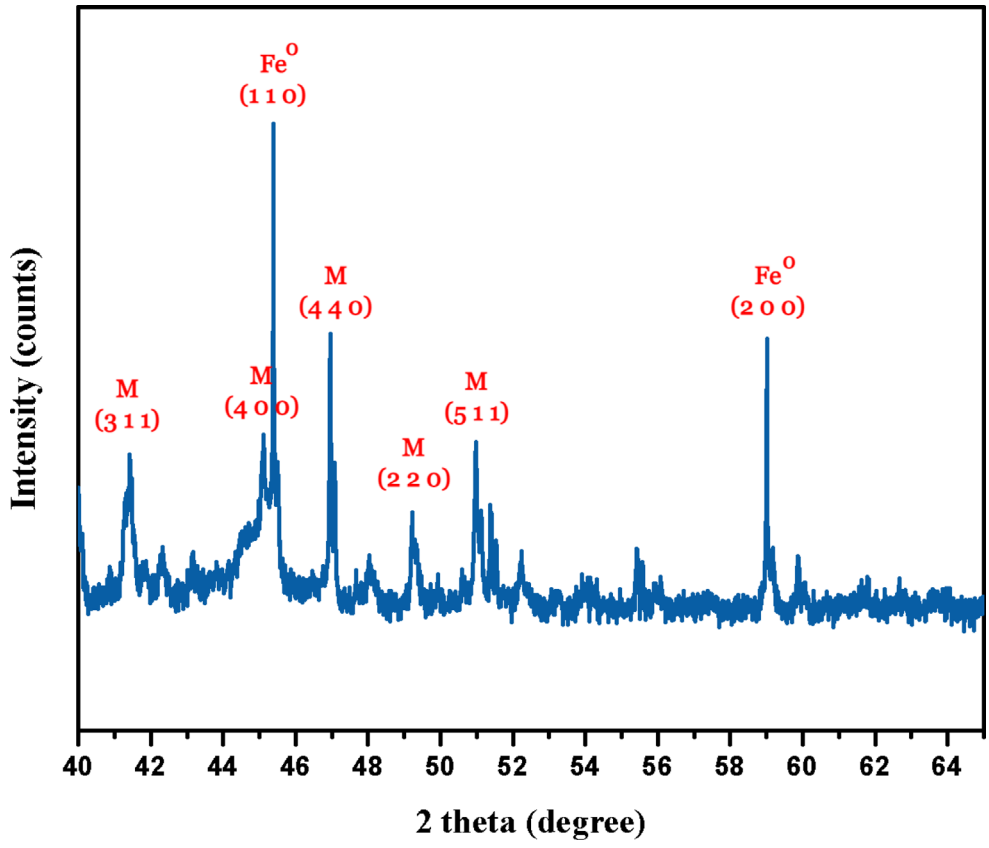

Figure 1. The XRD plot of the prepared nZVI particles [17, 18].

β stands for the full width at half maximum (FWHM) and θ is the Bragg's angle corresponding to the maximum peak intensity (obtained from 2θ). Accordingly, the mean crystalline grain size of nZVI was calculated to be 45.915 nm using the Scherrer equation, which is similar to previously reported literature data [18]. Additionally, the percentage of error from the Scherrer equation turns out to be 1.085%

FESEM (JEOL JSM-7600) was undertaken to qualitatively ascertain the spherical morphology, with subsequent formation of chain-like aggregates of our experimentally fabricated nZVI sample. Figures 2a and 2b show the SEM images of the synthesized nZVI. As a direct consequence of rapid oxidation to mixed valent iron oxides, the SEM images can be seen to develop unavoidable core-shell structure at certain points, formed over the highly reactive nZVI particles. This, however shields the zero-valent iron NPs, and prevents them from further oxidation. The spherical particles having a size distribution of 20–60 nm demonstrates the chain-like morphology, which might be attributed to the large surface area of individual particles and magnetic dipole-dipole interaction. Additionally, these oxidized components have also been reported to significantly affect the reactivity of nZVI in myriad of applications. The enormous surface area of this nZVI particle allows toxicants to be adsorbed better than its macroscopic counterpart.

Figure 2c shows TEM images of the prepared sample, with Figure 3 depicting the histogram plot of the obtained TEM images. Data from TEM analysis (JEM-2100, JEOL) reveals a similar facet to previously analyzed SEM images. Clearly visible irregular and spherical particles of dimensions ranging within 30–50 nm clearly matches with our SEM results. The varying texture of the core-shell structure from dusky to lighter shades distinctly differentiates the core and shell respectively, with the core representing the zero-valent iron NPs and the shell conforms to the presence of mixed-valent oxidized compounds- a result consistent with previously studied zero-valent iron NPs characterization.

Photodegradation of phenol was carried out using a 200 ml beaker. Batch mode operation was employed and the experiment was conducted at a temperature (25 ± 2 °C), a little below room temperature using UV/Vis spectrophotometer (Hitachi spectrophotometer U-4100, range: 240–2600 nm). The low temperature was so chosen to abstain the phenol from evaporation. Water and phenol were mixed in a 5:1 ratio and stirred vigorously to form water–phenol dispersion since phenol has very low solubility in an aqueous medium. 0.1 molar (nZVI) particles were added and the photodegradation study was reported in dark and light employing an AM 1.5 light source, which corresponds to a power of 100 mW/cm^2. To prohibit the settling down of the insoluble nanoparticles and the water

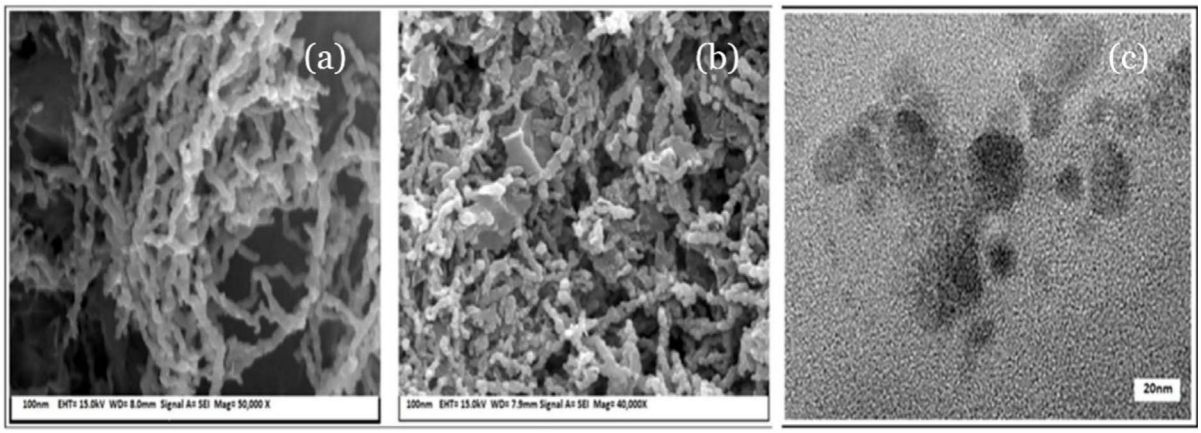

Figure 2. (a)–(b) FESEM of the nZVI characterization and (c) TEM images of the experimentally obtained nZVI particles.

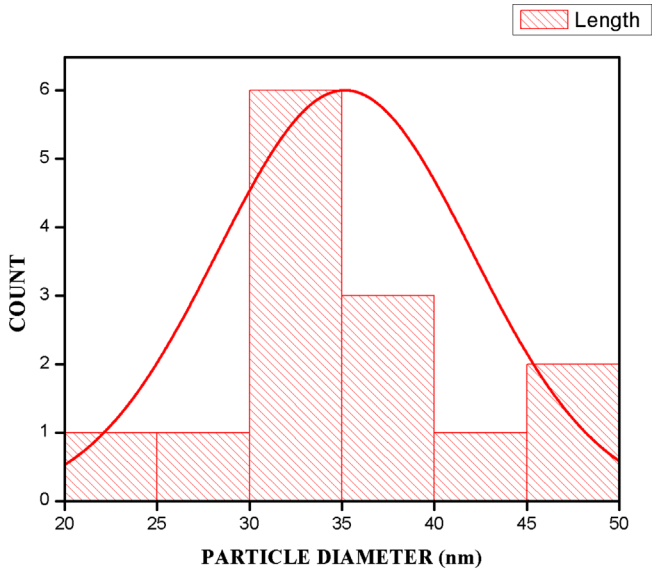

Figure 3. Histogram plot of the obtained TEM images.

phenol emulsion stirring was continued for the whole phase of the experiment. This additionally, increased the surface area available for interaction between the organic pollutant and the (nZVI) Powder. The experimentally obtained concentration profile of phenol is provided in Figure 4 and suggests the degradation phenomena only with the incident irradiation. No degradation in the concentration of phenol was observed in the dark phase.

The decreasing concentration of phenol was observed for 2 hr using a spectrophotometer. The Fenton or photo-Fenton process tends to be fairly effective with (nZVI) as the Fenton reagent, and a mixture of H_2O_2 and Fe^{+2} for phenol degradation in water [19]. Whereas the mechanism of reduction of organic pollutants on the (nZVI) surface is well documented, the nanoparticles may produce strong oxidating compounds, and oxidative degradation of the present organic pollutants also becomes a possibility. The latter mechanism happens with the help of OH^- radicals under oxic and acidic conditions thereby not recovering the addition of H_2O_2 which is a critical bottleneck to the use of (nZVI) as a photo degrading reagent.

As can be illustrated photodegradation plot, nearly 40% of the phenol was removed within the first 120 minutes, over which the removal initially was rapid and then plateaued after an hour. They employed an advanced oxidation process that was responsible for the creation of hydroxyl radicals which were subsequently accountable for the oxidation of the phenol in the aqueous medium. Subsequently, in conformation with previous literatures, catechol and hydroquinone can be estimated to be immediate products which finally results in the formation of carbon dioxide and water as the final degraded products of phenol.

Figure 5 depicts that the degradation kinetics of the Phenol–water solution follows the pseudo-first-order kinetics. The value of "**k**" (reaction rate const.) was calculated by fitting the data derived using the solution of the equation,

$$\frac{\mathrm{d}[C]}{\mathrm{d}t} = -k[c]. \tag{3}$$

The value of "k", which is the slope of the fitting curve, was found to be 0.00349 min^{-1}. The high value of R^2 (0.958) implicated the removal of Phenol using nZVI fitted well under the pseudo-first-order kinetics. Further, using the solution of the equation, it was found that 1392 min ($\sim$ 23.2 hr) is required to quantitatively remove 99% of Phenol from the Phenol–water solution. The catalyst retrieved after 120 min of the experimentation showed severe oxidation of the nZVI particles forming a large number of oxidized compounds on the shell, therefore shielding the nZVI particles of the core from taking part as a catalyst in further cycles. The following table shows a comparative study of various other compounds used for the photodegradation of phenol experiment.

A photoluminescence (PL) study (480 nm excitation from an air-cooled argon ion laser with a Peltier-cooled charge-coupled-device detector) of nZVI has been done since it is one the most promising way to find out the electronic property of any material. The relative difficulty of

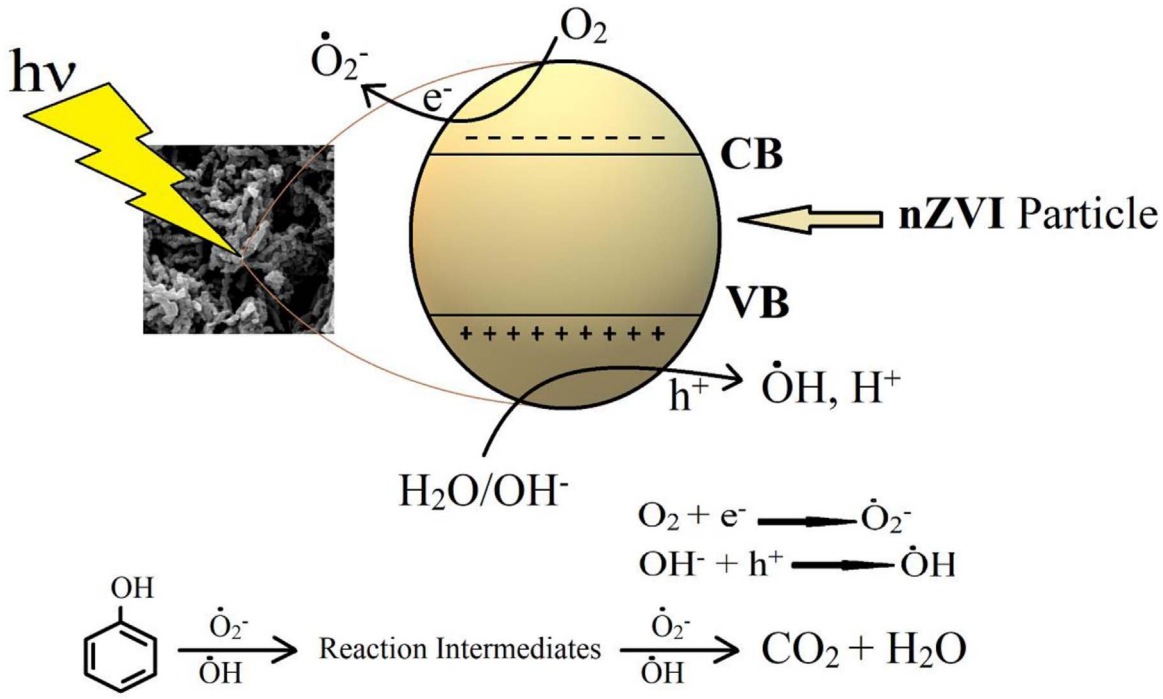

Figure 4. Mechanism of Phenol degradation using nZVI particle in presence of light.

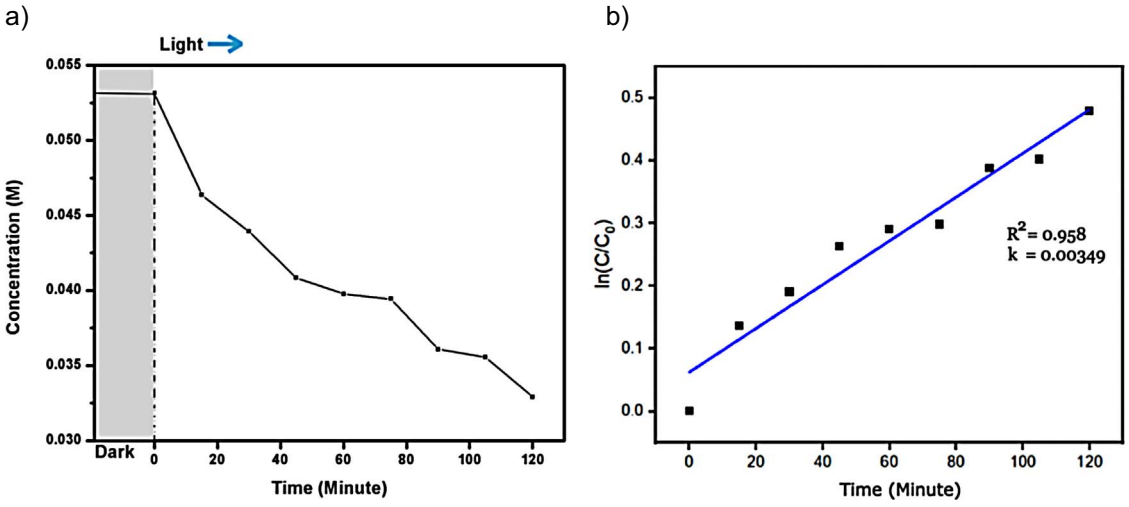

Figure 5. (a) Transient concentration profile of phenol with incident irradiation of AM 1.5, and (b) Kinetic study of the photodegradation mechanism by nZVI particles.

achieving a lowest energy transition, yet provide optical results for the material concerned requires PL documentation, which nevertheless provides an insight into the properties of our synthesized nZVI. An excitation wavelength of 480 nm was used to retrieve the PL spectra. Figure 6 represents the PL characteristics of the particle where a Gaussian fit has been performed which indicates the two distinct peaks at 670 nm and 720 nm [24] (Fig. 6).

The lowest energy transition of zero-valent iron NPs from the PL study are calculated using the following equation,

$$E_g = \frac{1240}{\lambda}\text{eV}. \quad (4)$$

Here, "$\boldsymbol{k}$" is the wavelength where the secondary peak, also known as emission spectra peak, is observed i.e., 720 nm. Therefore, the experimental lowest energy transition of nZVI, calculated from the PL study is approximately 1.72 eV which clearly states that zero-valent iron nanoparticles behave like semiconductors, whereas, Iron has inherent conductive properties.

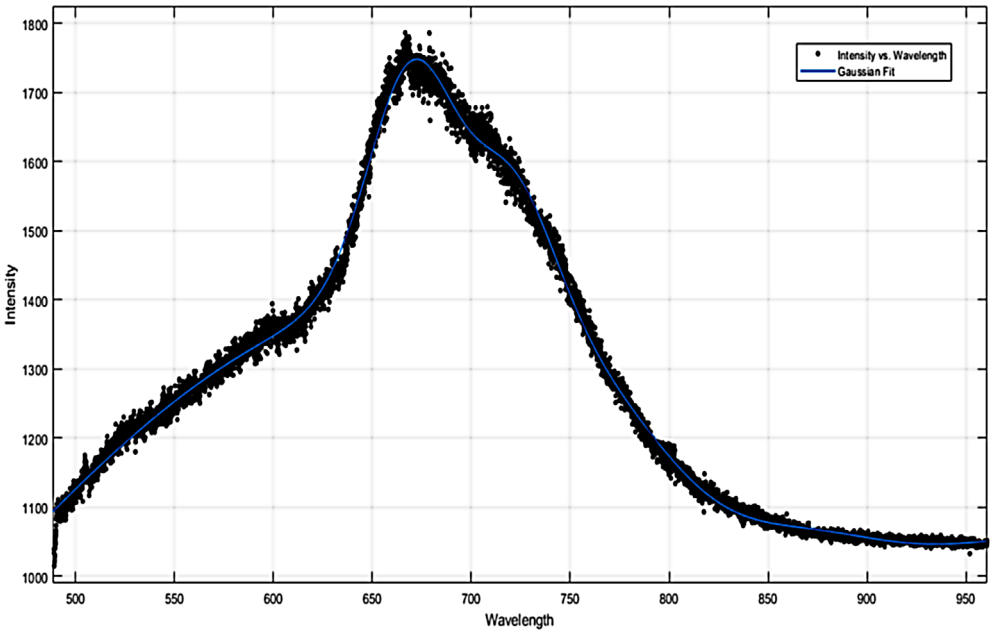

Figure 6. The photoluminescence spectra of Zero-valent iron nanoparticles.

Table 1. A comparative study of the reaction rate constant employing different photocatalyst.

Compound	Reaction rate constant (k)	R^2	Ref.
nZVI	0.00349 min^{-1}	0.958	This work
TiO_2	0.07–0.18 min^{-1}	0.99	[20]
Nano-ZnO	0.05 min^{-1}	0.992	[21]
Fe_3O_4	0.0003 min^{-1}	0.8141	[22]
Fe_3O_4–H_2O_2	0.0017 min^{-1}	0.8529	
Fe_3O_4–oxalate	0.0183 min^{-1}	0.9655	
Fe_3O_4–oxalate–H_2O_2	0.0190 min^{-1}	0.9852	
P123–TiO_2	0.0027 min^{-1}	0.9862	[23]
M18	0.0019 min^{-1}	0.9748	
CTAB-TiO_2	0.0018 min^{-1}	0.9864	

Additionally, this nanoparticle emits energy in the near IR and IR regions, thus this can be extensively used in wireless operations, sensing, and tracking technologies.

Conclusions

This research work focused on the synthesis of ZVI nanoparticles by chemical reduction where ethanol was used as the base medium. SEM and TEM characterization showed the presence of nanoclusters and an interlinked network. The XRD pattern has shown the formation of a pure crystalline phase, which however also depicted the presence of additional peaks due to oxidized Fe_2O_3 and Fe_3O_4. Photodegradation of phenol was studied under AM 1.5 illumination by using the synthesized nZVI sample as the photocatalyst. The photodegradation was solely carried out by abstaining from the use of H_2O_2 which is a crucial reagent for the reduction of organic pollutants. However, the absence of peroxide did not alter the oxidative mechanism of the nanoparticles and a 40% phenol degradation efficiency was achieved over 2 h. The enhanced removal capability can be attributed to the nanoparticles' higher surface area, as a result of which an increased surface reactivity may also be assumed. The PL spectra have yielded a lowest energy transition of 1.72 eV which has supported the photon absorption capacity of the synthesized NPs. As a result of which, nZVI can be expected to play a crucial role in wastewater treatment and groundwater remediation. The low energy transition also supports the application of nZVI in tracking technology, wireless operation, and optoelectronic devices.

Future work entails the kinetic study of the photodegradation mechanism under different simulated conditions. Operational parameters such as the initial concentration of phenol and nZVI in water, pH, temperature, and light intensity have been seen to play major roles and therefore can be tested on our formulation based on an ethanol medium. Furthermore, first-principle calculations can be carried out on the formulated nanoparticle to understand the inherent energy interactions within the iron nanoparticle that results in such enhanced performance over its bulk nature.

Acknowledgments

We also like to acknowledge Science and Engineering Research Board [SERB] grants funded by the Department of Science and Technology [DST] Central, Government of India through Teachers Associateship for Research Excellence [TAR/2018/000195] for providing financial support.

Conflict of interest

The authors declare that they have no conflict of interest.

References

1. Mondal S, Bera S, Mishra R, Roy S (2022), Redefining the role of microalgae in industrial wastewater remediation. Energy Nexus 6, 100088. https://doi.org/10.1016/j.nexus.2022.100088.
2. Pradeep NV, Anupama S, Navya K, Shalini HN, Idris M, Hampannavar US (2014), Biological removal of phenol from wastewaters: a mini review. Appl Water Sci 5, 105–112. https://doi.org/10.1007/s13201-014-0176-8.
3. Singh R, Misra V (2016), Stabilization of zero-valent iron nanoparticles: role of polymers and surfactants. Handbook of Nanoparticles 985–1007. https://doi.org/10.1007/978-3-319-15338-4_44.
4. Tarekegn MM, Hiruy AM, Dekebo AH (2021), Nano Zero Valent Iron (NZVI) particles for the removal of heavy metals (Cd2+, Cu2+ and Pb2+) from aqueous solutions. RSC Adv 11, 18539–18551. https://doi.org/10.1039/d1ra01427g.
5. Li S, Wang W, Liang F, Zhang W (2017), Heavy metal removal using Nanoscale Zero-Valent Iron (NZVI): Theory and application. J Hazardous Mater 322, 163–171. https://doi.org/10.1016/j.jhazmat.2016.01.032.
6. Almomani F, Bhosale R, Khraisheh M, Kumar A, Almomani T (2020), Heavy metal ions removal from industrial wastewater using Magnetic Nanoparticles (MNP). Appl Surf Sci 506, 144924. https://doi.org/10.1016/j.apsusc.2019.144924.
7. Ansari A, Siddiqui VU, Akram MK, Siddiqi WA, Sajid S (2020), Removal of Pb(II) from industrial wastewater using of CuO/Alg nanocomposite. Lect Notes Civ Eng 167–175. https://doi.org/10.1007/978-981-15-2545-2_16.
8. Fan M, Yuan P, Chen T, He H, Yuan A, Chen K, Zhu J, Liu D (2010), Synthesis, characterization and size control of zerovalent iron nanoparticles anchored on montmorillonite. Chin Sci Bull 55, 1092–1099. https://doi.org/10.1007/s11434-010-0062-1.
9. Jain K, Patel AS, Pardhi VP, Flora SJS (2021), Nanotechnology in wastewater management: a new paradigm towards wastewater treatment. Molecules 26, 1797. https://doi.org/10.3390/molecules26061797.
10. Stefaniuk M, Oleszczuk P, Ok YS (2016), Review on Nano Zerovalent Iron (NZVI): From synthesis to environmental applications. Chem Eng J 287, 618–632. https://doi.org/10.1016/j.cej.2015.11.046.
11. Roy S, Kargupta K, Chakraborty S, Ganguly S (2008), Preparation of polyaniline nanofibers and nanoparticles via simultaneous doping and electro-deposition. Mater Lett 62, 2535–2538. https://doi.org/10.1016/j.matlet.2007.12.066.
12. Ayranci E, Conway BE (2001), Removal of phenol, phenoxide and chlorophenols from waste-waters by adsorption and electrosorption at high-area carbon felt electrodes. J Electroanal Chem 513, 100–110. https://doi.org/10.1016/s0022-0728(01)00529-0.
13. Zhang J, Zhuang J, Gao L, Zhang Y, Gu N, Feng J, Yang D, Zhu J, Yan X (2008), Decomposing phenol by the hidden talent of ferromagnetic nanoparticles. Chemosphere 73, 1524–1528. https://doi.org/10.1016/j.chemosphere.2008.05.050.
14. Jamei MR, Khosravi MR, Anvaripour B (2013), Investigation of ultrasonic effect on synthesis of nano zero valent iron particles and comparison with conventional method. Asia-Pac J Chem Eng 8, 767–774. https://doi.org/10.1002/apj.1720.
15. Adusei-Gyamfi J, Acha V (2016), Carriers for Nano Zerovalent Iron (NZVI): Synthesis application and efficiency. RSC Adv 6, 91025–91044. https://doi.org/10.1039/c6ra16657a.
16. Taha MR, Ibrahim AH (2014), Characterization of Nano Zero-Valent Iron (NZVI) and its application in sono-fenton process to remove COD in palm oil mill effluent. Journal of Environmental Chemical Engineering 2, 1–8. https://doi.org/10.1016/j.jece.2013.11.021.
17. Fan J, Guo Y, Wang J, Fan M (2009), Rapid decolorization of azo dye methyl orange in aqueous solution by nanoscale zerovalent iron particles. J Hazardous Mater 166, 904–910. https://doi.org/10.1016/j.jhazmat.2008.11.091.
18. Elshafai M, Hamdy A, Hefny MM (2018), Zero-valent iron nanostructures: synthesis characterization and application. J Environ Biotechnol Res 7, 1, 1–10.
19. Shimizu A, Tokumura M, Nakajima K, Kawase Y (2012), Phenol removal using zero-valent iron powder in the presence of dissolved oxygen: roles of decomposition by the Fenton reaction and adsorption/precipitation. J Hazardous Mater 201–202, 60–67. https://doi.org/10.1016/j.jhazmat.2011.11.009.
20. Dang TTT, Le STT, Channei D, Khanitchaidecha W, Nakaruk A (2016), Photodegradation mechanisms of phenol in the photocatalytic process. Res ChemIntermed 42, 5961–5974. https://doi.org/10.1007/s11164-015-2417-3.
21. Tao Y, Cheng ZL, Ting KE, Yin XJ (2013), Photocatalytic degradation of phenol using a nanocatalyst: the mechanism and kinetics. J Catalysts 2013, 1–6. https://doi.org/10.1155/2013/364275.
22. Xu P, Zeng G, Huang D, Liu L, Lai C, Chen M, Zhang C, Lai M, He Y (2014), Photocatalytic degradation of phenol by the heterogeneous Fe_3O_4 nanoparticles and oxalate complex system. RSC Adv 4, 40828–40836. https://doi.org/10.1039/c4ra05996d.
23. Nguyen TH, Vu AT, Dang VH, Wu JC-S, Le MT (2020), Photocatalytic degradation of phenol and methyl orange with titania-based photocatalysts synthesized by various methods in comparison with ZnO–graphene oxide composite. Top Catal 63, 1215–1226. https://doi.org/10.1007/s11244-020-01361-5.
24. Reichman J (2000), Handbook of optical filters for fluorescence microscopy, Chroma Technology Corporation.

Cite this article as: Shaikh A, Bera S, Paul S, Mondal S, Saha A, et al. 2022. Synthesis and characterization of Inorganic Nanoparticles Luminophores for Environmental Remediation. 4open, **5**, 19.